energies

MDPI

Article

Experimental Investigation to Assess the Performance Characteristics of a Marine Two-Stroke Dual Fuel Engine under Diesel and Natural Gas Mode

Theofanis D. Hountalas [1], Maria Founti [1] and Theodoros C. Zannis [2,*]

[1] Thermal Engineering Section, School of Mechanical Engineering, National Technical University of Athens, Zografou Campus, 15772 Athens, Greece; thountalas92@gmail.com (T.D.H.); mfou@central.ntua.gr (M.F.)
[2] Naval Architecture and Marine Engineering Section, Hellenic Naval Academy, 18539 Piraeus, Greece
* Correspondence: thzannis@hna.gr; Tel.: +30-2104581663

Abstract: With the aim of CO_2 emissions reduction in the maritime sector, dual fuel engines operating on natural gas are the most prominent technical and commercially available solution. A promising variant is the two-stroke high-pressure natural gas injection engine, utilizing diesel pilot fuel injection for ignition of the gaseous fuel while being able to operate in diesel-only mode. In this study, a comparative analysis of the performance and the combustion mechanism of dual fuel and diesel mode for this engine type is conducted using experimental data. Studies based on measurements conducted on actual scale are limited in the literature due to the engines' sheer size not allowing lab testing. The analysis was conducted using measurements acquired during the factory acceptance tests involving conventional operating data and cylinder pressure data acquired using a piezoelectric sensor. In terms of the mean pressure and temperature, only minor differences were found. The specific fuel consumption was improved under low load operation for the dual fuel mode by 1.8%, while a small increase of 1.2% was found near full load. Differences were found in the combustion process from 25 to 75% load with considerably faster premixed and diffusion combustion for the dual fuel mode leading to a 6–8% decrease in combustion duration. Despite the combustion process differences, the performance under dual fuel operation was overall close to that of conventional diesel with an acceptable 1.5% efficiency reduction on average. This confirms that modern dual fuel marine engines can achieve the performance standards of conventional ones while benefiting from low-carbon fuel use to reduce CO_2 emissions.

Keywords: high pressure; LNG; gas; injection; marine; engine; combustion; two stroke; diesel

Citation: Hountalas, T.D.; Founti, M.; Zannis, T.C. Experimental Investigation to Assess the Performance Characteristics of a Marine Two-Stroke Dual Fuel Engine under Diesel and Natural Gas Mode. *Energies* **2023**, *16*, 3551. https://doi.org/10.3390/en16083551

Academic Editor: Gabriele Di Blasio

Received: 7 March 2023
Revised: 12 April 2023
Accepted: 17 April 2023
Published: 19 April 2023

1. Introduction

The control of CO_2 emissions is at the core in the implementation of the decarbonization roadmap of the transportation industry. For the marine industry, the International Maritime Organization (IMO) has declared the aim to cut down the carbon emissions of marine vessels by 40% by 2030 and 70% by 2050 compared to 2008 [1]. In addition to CO_2, considerable quantities of pollutants toxic to human health are emitted from vessels [2]. These affect air quality, and various fuel types, such as biofuels, are currently under investigation regarding their impact on these pollutants' emissions [3]. The technological solutions to be adopted for a carbon-free future for the marine sector are yet to be decided, since further research is required. However, there is a consensus among a large part of the industry that an intermediate step for the next decades, preceding total carbon-free solutions, is the use of low-carbon fuels [1,4]. The main bottleneck with low-carbon fuels is their general and local availability and the associated overall distribution across bunkering facilities in the world. The production and availability of natural gas and readiness for use in the marine sector are maturing at a strong pace [4]. Currently, the low-carbon fuel with the highest adoption by ship owners is natural gas [5]. Natural gas marine engines

operate on a dual fuel basis, using liquified natural gas (LNG) as the main fuel and a small quantity of diesel fuel or a crude oil variant as the ignition source in the form of a short pilot injection. Low-pressure and high-pressure gas injection are the two leading approaches for LNG injection and combustion, both with broad market availability. The present study investigates the high-pressure two-stroke dual fuel variant performance. These engines are equipped with two sets of injectors, one for LNG and one for diesel fuel. LNG injection occurs near the top dead center (TDC), with timing similar to that of the diesel fuel pilot. The advantage over the low-pressure induction approach is increased efficiency [6], leading to lower fuel consumption, almost zero particulate emissions [7] and higher stability under low load operation, which is important when maneuvering near populated areas. An additional advantage is the compression of air instead of a natural gas and air mixture, which reduces concerns over methane slip and safety due to leakages and blowby. The disadvantages of this approach are the complexity and additional cost of the LNG high-pressure gas injection equipment. In addition, the resulting NO_x emissions are comparable to those of conventional diesel fuel marine engines, in contrast to low-pressure gas induction engines, which are Tier III compliant [8,9]. NO_x emissions are highly toxic and are a pollutant controlled by the IMO [10]. Since they are a by-product of the combustion process, either internal and/or external measures are used for their control to achieve the applicable emission limits [11]. The requirement for additional equipment for NO_x emissions control compared to low-pressure gas engines further increases the initial investment cost and operational cost [9]. The main similarity of the high-pressure natural gas injection to conventional diesel operation is that both fuels are injected close to the TDC. The diesel pilot acts as the means for ignition of the NG injected simultaneously or shortly before/after depending on the engine configuration [12]. Thus, the combustion in this case is expected to be mostly diffusion controlled, as in the typical diesel engine [13]. This is in contrast to the low-pressure gas induction system where natural gas is injected in the cylinder early in the compression stage, so it is allowed adequate time to mix with air [14] and operates on a lean burn mixture principle [15]. While these are currently the main solutions utilized in the marine sector, several other solutions are being investigated in other parts of the internal combustion engines field, such as the use of ethanol and hydrogen fuels [16,17], which can potentially be adopted by the marine industry in the future. Currently, NH_3 as a hydrogen carrier is also examined by engine makers [18].

In the present work, the operation of a dual fuel high-pressure gas injection engine is examined under both diesel and dual fuel modes, referred to as a DF mode thereafter. The basis for the analysis is cylinder pressure traces acquired from the engine's cylinders for six load points ranging from 25 to 110% under both operating modes. The specific engine was equipped with an exhaust gas recirculation (EGR) system and was capable of operating under both Tier-II and Tier-III modes. Due to space restrictions, only the performance and combustion data are examined in the present work. The emissions data will be provided in detail in a future communication, where the results of the Tier-III mode will also be included.

The objective of the study is to evaluate the differences in overall performance between the diesel and DF modes. The general engine behavior is examined, and the focus is directed toward comparing the differences in the combustion process due to the use of LNG and pilot diesel fuel injection for ignition. A direct comparison of the two modes utilizing actual measurement data from this engine type in a controlled environment and without the use of a simulator is challenging due to significant constraints in the measurement procedure for these engines. The constraints result mainly from the sheer size, fuel consumption and power output of the engine, which prohibits testing in a laboratory environment, and the limited availability of vessels' schedule to allow for lengthy measurement procedures along with the various challenges of conducting on-board tests. Thus, at the time of this study, comparisons of the two-stroke high-pressure gas injection engines using experimental data are scarce in the literature, especially when considering the experimental data for both diesel and gas modes under various loads.

Most of the available information is based on simulation results and commonly refers to four-stroke or low-pressure gas injection engines, as detailed below. The majority of research works employ the use of computational methods.

One approach is the use of CFD simulation of fuel and gas injection and combustion, as in the case of Refs [19,20]. Both works confirm the expectation of a fast and intense fuel burn rate of methane, which is visible in the fuel burn rate diagrams. Additionally, in Ref [19], the influence of the pilot injection and ignition angle is evaluated regarding its effect on combustion intensity, which generally increases with pilot injection delay. Investigations based on the utilization of experimental data from direct gas injection engines are provided in Ref [21], but no information is available for two-stroke marine engines. The use of experimental data and analysis with simulation software is utilized in Ref [22] to investigate the combustion characteristics of diesel and gas modes. An intense combustion of NG is found, with most of the gas fuel burning during the rapid combustion phase, resulting in an overall lower combustion duration, which is in agreement with the general findings of the present work. Further results based on experimental data are reported in a review of various types of marine dual fuel engines in Ref [23]. In these investigations, a significant effect of the dual fuel combustion mechanism on the heat release rate mechanism is revealed. The effect is similar to the one predicted by the aforementioned CFD simulation works. For low-pressure gas induction, the marine dual fuel engines that are examined in Refs [24,25] which are also mainly computational. The results are not comparable to the high-pressure direct gas injection variant, as fuel mixing and, consequently, the combustion process, differ significantly.

For the present work, acquisition of the experimental data under both diesel and gas modes from full scale testing was achieved by conducting the measurement procedure alongside the process of the engine's factory acceptance tests at the engine manufacturer's facility. This provided a controlled environment with high-quality instrumentation and the same conditions for the testing of both modes. With this approach, high-quality experimental data were acquired and used to conduct a full comparative investigation of the two modes using the actual engine under normal operation, providing insight into the studied subject using measurement data, which were hitherto limited in peer-reviewed work. In addition to the recorded data, engine settings were determined using an analysis conducted with the aid of a diagnosis software [26]. This step is important, as tuning between single and dual fuel mode differs for these engines by design. The two modes' individual tuning settings are compared, and their effect on engine performance is examined in tandem with the fuel effect achieved. The acquired cylinder pressure traces were processed to derive the heat release rate, which was used to conduct an analysis of the combustion process. The estimated heat release rate was used to determine the effect of natural gas use on combustion progression, intensity and combustion duration in comparison to the corresponding values of the diesel mode, which are the areas expected to be most affected based on the available literature detailed above.

2. Testing Procedure and Particulars

The measurements were performed during the factory acceptance test procedure of a high-pressure NG injection dual fuel two-stroke marine engine. The testing involved operation under natural gas dual fuel mode using marine diesel and natural gas and operation under a diesel-only mode. All engine operating parameters were recorded during the test procedure, along with the control system commands to the engine, using the engine control room instrumentation. The main operating parameters obtained were the following:

- Ambient conditions (temperature, pressure, humidity);
- Engine brake power;
- Diesel fuel and natural gas fuel consumption;
- Engine fuel index value: diesel and gas;
- Scavenging air pressure and temperature;

- Cylinder exhaust gas temperatures;
- T/C data: speed and pressure/temperature at inlet and outlet;
- Air cooler data: pressure and temperature of air and cooling water at inlet and outlet;
- Information on start of injection (SOI), exhaust valve opening (EVO) angle and exhaust valve closing (EVC) angle.

The studied engine is electronically controlled, and each cylinder is fitted with a piezoelectric pressure sensor on the cylinder head, which is used for control and monitoring by the engine's control system [27]. These piezoelectric sensors are designed for prolonged high-temperature operation by Kistler AG. The sampling rate used for the cylinder pressure measurement was 0.5° crank angle, achieved using an encoder mounted on the engine crankshaft. The cylinder pressure signal is continuously recorded simultaneously for all cylinders. A simplified schematic of the engine control system is provided in Figure 1. A minimum of 40 engine cycles were recorded for each measurement, and the mean cycle was used for the analysis. This was found adequate for low-speed two-stroke engines when accounting for load variation and other effects of sporadic phenomena [28]. The data presented below, including the pressure traces and temperature values, are the mean values from all cylinders depicting the total engine state. From the analysis, it was confirmed that the operation was uniform for all engine cylinders.

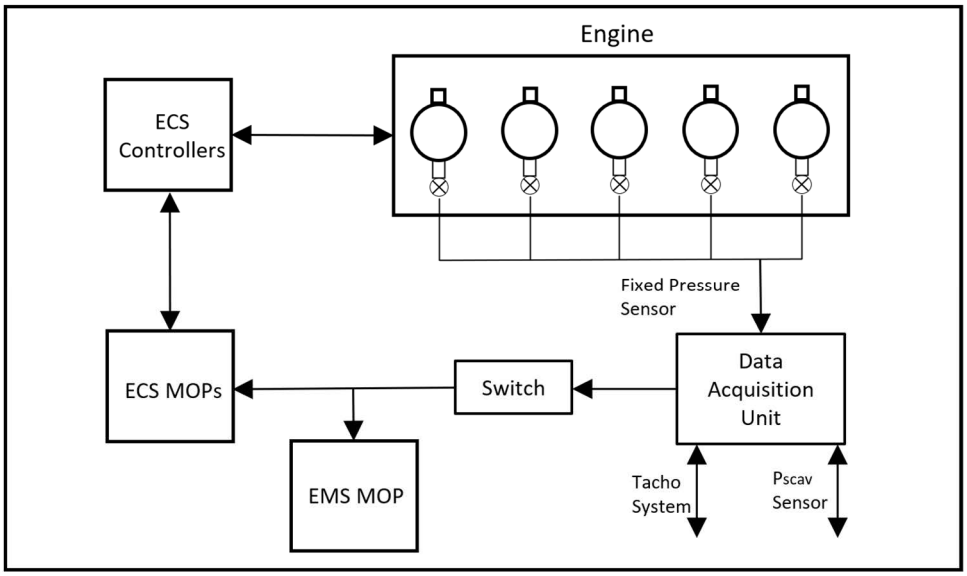

Figure 1. Engine control system schematic, simplified.

The engine particulars, as well as the diesel and natural gas properties, are provided in Tables 1–3. A schematic of the measurement layout is provided in Figure 2.

Table 1. Engine particulars tested.

5G70ME-C9.5GI	Units	Value
Type	-	Two-stroke
Electronic Control	-	Yes
Cylinder No.	-	5
Bore	mm	700
Stroke	mm	3256
Nominal Speed	rpm	68.1
Nominal Power	kW	11,975

Table 2. Diesel fuel and natural gas properties.

Diesel Fuel Properties	**Units**	**Value**
Density at 15 °C	kg/m^3	879.00
Lower Calorific Value	kcal/kg	10,116.00
Viscosity at 40 °C	cSt	5.98
Sulfur (m/m)	%	0.16
Carbon (m/m)	%	86.70
Natural Gas Properties	**Units**	**Value**
Methane (CH_4)	% mol	86.60
Ethane (C_2H_6)	% mol	9.89
Lower Heating Value	kcal/kg	11,762.00
Total Carbon (m/m)	%	76.30

Table 3. Characteristics of instrumentation for engine performance monitoring.

Instrument	**Measured Parameter**	**Range**	**Accuracy**
Hydraulic Brake	Torque Speed	0–250 rpm	<0.5% 0.1 rpm
Diesel Fuel Scale	Diesel Fuel Consumption	0–10,000 kg	0.2%
Gaseous Fuel Scale	Gas Fuel Consumption	0–10,000 kg	0.3%
MBS 3000	Scavenging Air Pressure	0–10 bar	0.5%
Air Temperature Sensors	Scavenging Air Temperature	−10–80 °C	0.2 °C
Exhaust Gas Temperature Sensors	Exhaust Gas Temperature	−10–700 °C	0.5 °C
Cooling Water Temperature Sensors	Cooling Water Temperature	0–180 °C	0.2 °C
Kistler 6613CG2	In-Cylinder Pressure	0–250 bar	±0.5 bar

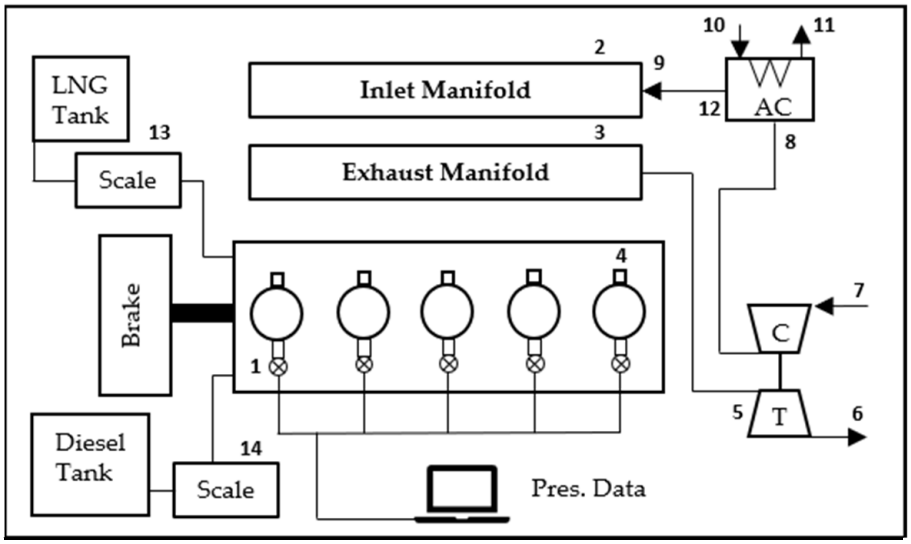

1. Cylinder Pressure Trace
2. Scavenging Pressure
3. Exhaust Pressure
4. Cylinder Exhaust Gas Temp.
5. Turbine Inlet Temp.
6. Turbine Outlet Temp.
7. Compressor Air Inlet Temp.
8. Air Temp. before Cooler
9. Air Temp. after Cooler
10. A/C Water Temp. In
11. A/C Water Temp. Out
12. A/C Pressure Drop
13. NG Consumption
14. Diesel Consumption

Figure 2. Measurement layout schematic.

Table 3 provides the particulars of the instrumentation used. Since the procedure was conducted at the maker's facility during the engine's certification FATs, the instrument state, calibration and measurement procedure are considered optimal.

2.1. Analysis of Measured Data

Processing of Measured Cylinder Pressure Data

The most valuable source of information for the evaluation of dual fuel performance and comparison with a typical diesel mode is the cylinder pressure trace. Using the cylinder pressure data recorded, the following information was derived using an advanced diagnostic technique described in detail in Refs [29,30].

- Engine brake power: Estimated from the indicated power using the mechanical efficiency map of the engine defined during the shop test procedure. The power is compared against the one measured using the hydraulic brake to evaluate the quality and accuracy of the measured pressure data.
- Combustion rate of fuel: Estimated by applying the heat release rate analysis methodology described below.
- Start of combustion: The ignition angle was estimated from the cumulative heat release from the point where 3% of total heat was released. For verification of the derived values, a second methodology was used based on the second derivative of cylinder pressure to crank angle.
- Start of injection: Estimated from the ignition angle and the correlation used to derive the ignition delay [31]. The value was cross-referenced with the ECS indication.
- Exhaust valve opening (EVO): This value is directly provided by the ECS and is secondarily estimated for verification from the measured cylinder pressure trace using a technique described in Refs [29,30]. The latter is based on the simulation of the expansion stroke after combustion end using the closed cycle assumption.
- Exhaust valve closing (EVC) angle: This value is provided indirectly by the exhaust valve actuator signal, which is available in the ECS. The value is verified using an engine simulation model to match the measured P_{comp}/P_{scav} value, as described in Refs [29,30].

2.2. Estimation of Combustion Rate

The burn rate of fuel provides information on the combustion process, which is of major interest for dual fuel operation. It allows a study of ignition, combustion progression and duration, which are expected to differ when using a high-ignitability pilot fuel and a low-ignitability main fuel injected in parallel inside the combustion chamber. The fuel burn rate is derived by conducting a heat release rate analysis of the measured cylinder pressure traces. The process to estimate the net heat release rate is based on the first thermodynamic law [32]:

$$\frac{dQ_{net}}{d\varphi} = \frac{C_v}{R}\left(P\frac{dV}{d\varphi} + V\frac{dP}{d\varphi} - \frac{PV}{m}\frac{dm}{d\varphi}\right) + P\frac{dV}{d\varphi}, \quad (1)$$

In the above equation, the following assumptions are made:

- The cylinder contents are assumed to behave as an ideal gas, which is close to reality.
- The cylinder mass is considered constant, which does not present an accuracy reduction due to the extremely low blow-by rate of the tested engine, as revealed in the performance analysis.
- Uniform distribution of the thermodynamic properties inside the combustion chamber.
- The composition of cylinder content charge variability is estimated using the initial mass after EVC and the amount of fuel burnt from the heat release rate analysis and the measured fuel consumption. For this purpose, an iterative procedure is used until the convergence of the total estimated fuels amount with the measured ones using the known heating value of the fuels [29].

For the estimation of engine fuel consumption and the actual fuel combustion rate, it is necessary to use the gross heat release rate. This is provided in Ref [32]:

$$\frac{dQ_{gross}}{d\varphi} = \frac{dQ_{net}}{d\varphi} - \frac{dQ_w}{d\varphi} \tag{2}$$

The heat loss rate $\frac{dQ_w}{d\varphi}$ is estimated using the heat transfer model of Annand [33], which has been found accurate in multiple similar applications for this engine type.

$$\frac{dQ_w}{d\varphi} = A\left(a_c\frac{\lambda}{D}Re^b\left(T_w - T_g\right) + c_r\left(T_w^4 - T_g^4\right)\right) \tag{3}$$

The heat transfer model is calibrated using the shop test data for which the measured cylinder pressure traces under 25%, 50%, 75% and 100% load along with accurate fuel oil consumption (FOC) data are available. For the heat release rate analysis, the mean cylinder gas temperature is used, calculated using the ideal gas law assumption:

$$T_g = \frac{PV}{mR} \tag{4}$$

The initial charge mass after EVC is estimated using a simulation model embedded in the diagnostic software utilizing an open cylinder simulation and the filling–emptying method [29]. The accuracy of the methodology is validated using the exhaust gas and air mass flow rates, which are determined using the carbon balance methodology and are available in the official NO_x file documentation of the engine.

3. Results and Discussion

In this section, the measurement data and subsequent analysis findings are presented. In addition, the key operating parameters of the engine under diesel and DF modes are provided.

3.1. General Performance Values

The overall engine performance differences between diesel and DF modes are presented herein. The mean compression pressure, peak combustion pressure and cylinder exhaust gas temperature for natural gas and diesel operation are compared in Figure 3a,b and Figure 4a, respectively. Initially, significant differences could be expected due to the use of pilot diesel injection for ignition and the properties of the natural gas fuel, mainly the energy content, which is significantly above that of conventional marine diesel. As revealed by the analysis, this expectation was not verified by the results. The differences are minimal for combustion pressure and exhaust gas temperature. Thus, no effect is expected on exhaust system components and the turbocharger during dual fuel mode operation. Regarding maximum pressure, the highly similar values indicate an effort by the engine manufacturer to maintain these values steady between the two modes via engine tuning. Differences are observed for the compression pressure (Figure 3b), which are mainly the result of P_{scav} differences. The specific engine type features variable exhaust valve timing; thus, the P_{comp} differences are also attributed to closing angle variation, as shown below in Section 3.2. The engine settings that affect the main operating parameters, namely the start of injection, exhaust valve opening/closing angle and air mass flow, also have a significant effect on exhaust gas temperature.

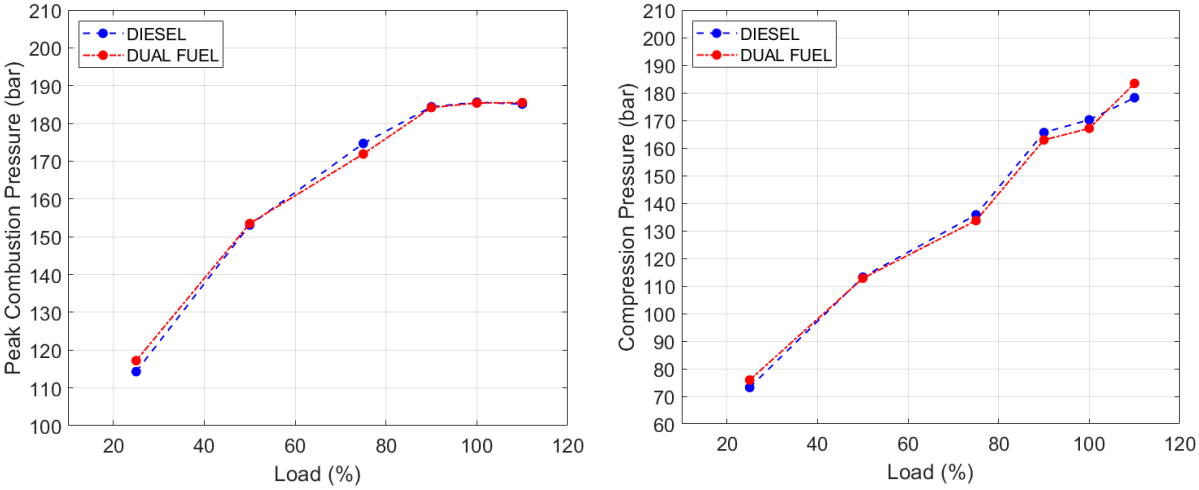

Figure 3. (**a**) Mean peak combustion pressure, diesel and DF modes; (**b**) Mean peak compression pressure, diesel and DF modes.

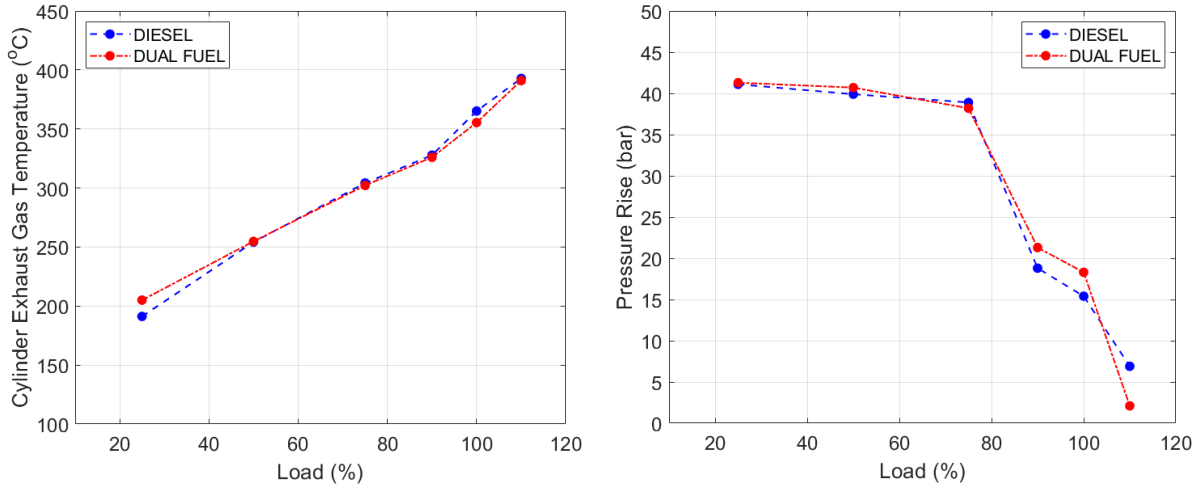

Figure 4. (**a**) Mean cylinder exhaust gas temperature, diesel and DF modes; (**b**) Pressure rise due to combustion, diesel and DF modes.

The compression pressure differences (Figure 3a) are reflected in the pressure rise due to combustion between the two modes (Figure 4b), as the peak combustion pressure (P_{max}) values are almost identical. For both modes, a steep decrease in pressure rise is observed as the load increases. Differences between the two modes are observed under a 90% load and above affected by the compression pressure values. The diesel and natural gas consumptions are provided in Figure 5a,b in kg/h. The differences in absolute values are mainly due to the calorific values of the two fuels, since the mass flow rates were not normalized to the same LCV. The total hourly fuel mass flow rate is higher for the diesel mode. On average, 12.9% more total fuel mass is consumed in the diesel mode, and this percentage remains mostly steady with the engine load. The diesel to natural gas mass ratio under a DF mode operation is provided in Figure 5c. The peak value is 14.53% under 25% load, and it gradually decreases to 5.16% under 100% and 110% loads. The previous ratio expressed in energy content results in 12.48% and 4.43%, respectively. According to the manufacturer, higher percentages are expected for very low load operation, up to the threshold for switchover to the diesel mode [27]. In Figure 5d,e, the ISO corrected SFC for the two modes is shown. For the DF mode, the SFC of the diesel pilot decreases

steadily, with the minimum value observed under maximum load, and the reverse is found for natural gas. For the diesel mode, the minimum SFC value is observed under a 50% load operation. The highest value is observed for the lowest load tested, 25%, which is normal under a low load due to deterioration of the mechanical efficiency. The most important parameter for long-term engine operation, also considering its size and CO_2 emissions, is specific fuel consumption (SFC). Due to the difference in LCV, the evaluation between the two modes in terms of efficiency cannot be based on the comparison of specific fuel consumption (SFC) without LCV corrections. For this reason, for the comparison of the two operating modes, the use of the total heat rate (THR) of both fuels consumed in (kJ/kWh) is preferred, as shown in Figure 5f. The total heat rate was calculated as follows:

$$\mathrm{THR} = \mathrm{SPC_{iso}} * \mathrm{LCV_{diesel}} + \mathrm{SGC_{iso}} * \mathrm{LCV_{gas}}, \quad (5)$$

Based on Figure 5f, the overall efficiency of the diesel mode is found to be higher, with lower total heat rate required for the same power output by the engine; however, the average difference is low. The efficiency gains under a diesel mode are mainly found in the region of 50% load and under maximum load. The average increase was calculated at 1.15%. In contrast, advantage in efficiency for the DF mode is observed under low load operation (25% load) at 1.82%. The accuracy of the previous calculation is the same as the accuracy of the fuel consumption values measured in the factory acceptance tests, which is higher than the level of difference observed and is thus reliable. Considering the mean values, only a small reduction in efficiency is observed for the DF mode, which is in the range of 1%. Further study of the performance under lower loads, below 25%, would be of interest, as the pilot fuel energy fraction increases significantly [27]; this was not feasible during the factory acceptance tests procedure, as in all cases, the load point tests begin at 25%. The findings of other studies regarding fuel consumption efficiency for marine high-pressure NG engines are summarized in Ref [23]. Different results can be found depending on the engine type and tuning, such as Refs [34,35]. Overall, modern dual fuel high-pressure engines are capable of similar efficiency as diesel engines under the selected load regions. Using the values of total gas and liquid fuel mass consumed and the carbon content of the fuels, as provided in Table 2, the CO_2 emissions of both modes can be estimated. This results in an almost steady 22.6% improvement under the DF mode, which is considerable.

These initial observations are analyzed along with the engine settings and operating conditions in the following section.

3.2. Comparative Evaluation of Engine Settings

In the present section, the engine settings are presented and compared for diesel and DF modes. The injection timing of diesel fuel and exhaust valve opening/closing angles, as well as the resulting compression ratio, are provided. These values were estimated from the processing of the cylinder pressure data using a well-tested diagnostic software [26] and cross-references with the ECS indications. The exhaust valve opening angle variation with load is found to be negligible for both modes. The absolute values are found to be identical for both modes (Figure 6a), showing identical tuning. This is important, as it confirms that exhaust gas temperatures, also found to be nearly identical, were not affected by valve timing. The exhaust valve closing angle variation with load is intense for both modes (Figure 6b), in contrast with the mostly steady opening angle timing. The analysis revealed small differences in exhaust valve closing angle timing between the DF and diesel modes. The valve closing angle is slightly delayed under DF mode operating at 50% load and below; for higher loads, the values are identical up to 100% load, and finally, the closing angle is advanced at 110% load. The resulting actual compression ratio (expressed using P_{comp}/P_{scav}) (Figure 6c) was affected by these variations, with decreased values for the 25% and 50% loads and increased value for the 110% load. The EVC timings do not result in significant differences in P_{comp} values (Figure 3b), except in the case of the 110% load. This latter difference is used to control peak combustion pressure in the DF mode and not to exceed the maximum permissible value. The alternative solution would be to delay fuel

injection, but this would have a higher negative impact on engine efficiency (SFC) than the one observed. The slight efficiency reduction already confirmed for this load, 110%, is of minimal impact, as the engine is not expected to operate under this load, except in emergency cases.

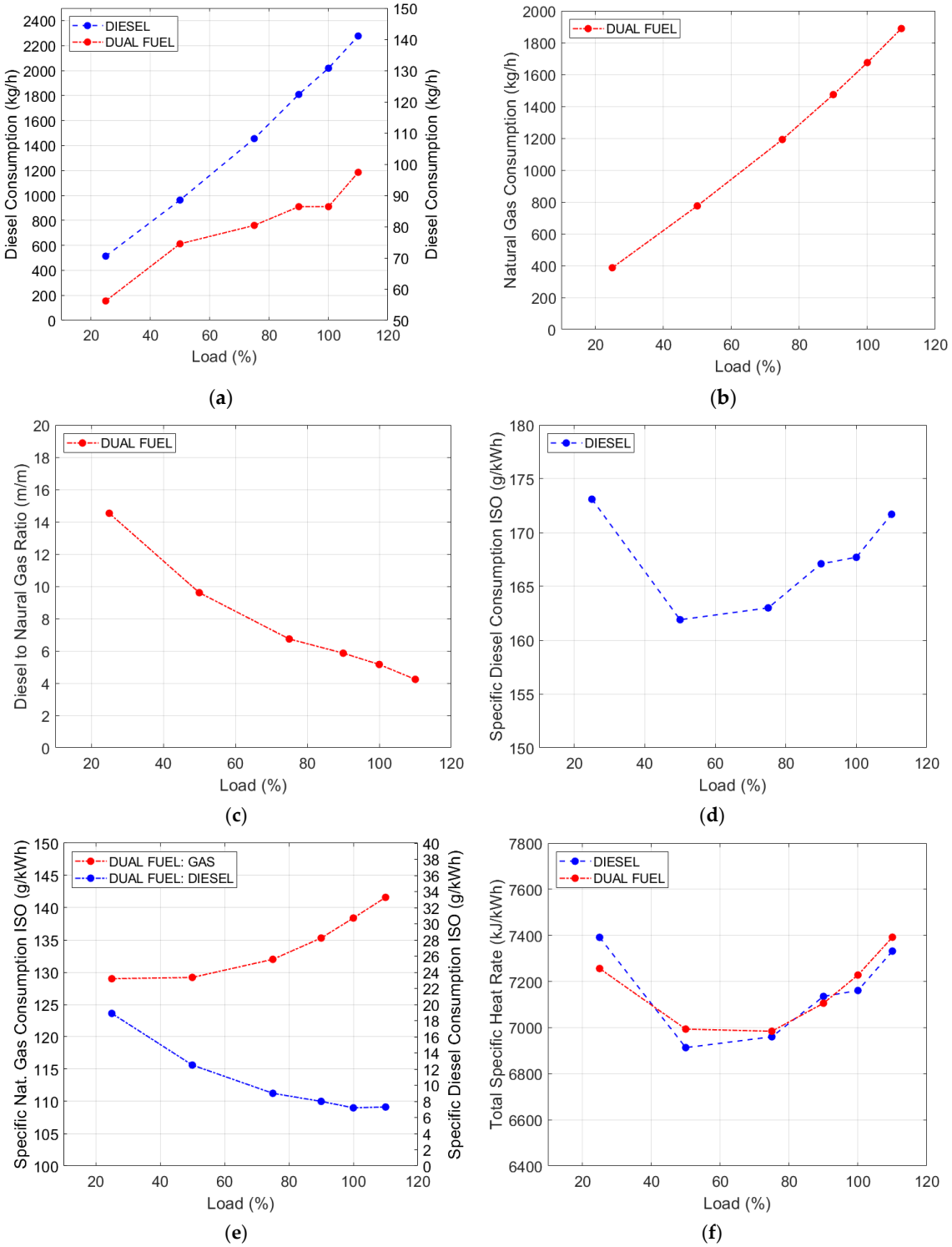

Figure 5. (**a**) Diesel consumption, diesel and DF modes; (**b**) Natural gas consumption, DF mode; (**c**) Mass ratio of diesel to natural gas; (**d**) Specific fuel consumption ISO, diesel mode; (**e**) Specific natural gas and diesel consumption ISO, DF mode; (**f**) Cumulative specific heat rate, diesel and DF modes.

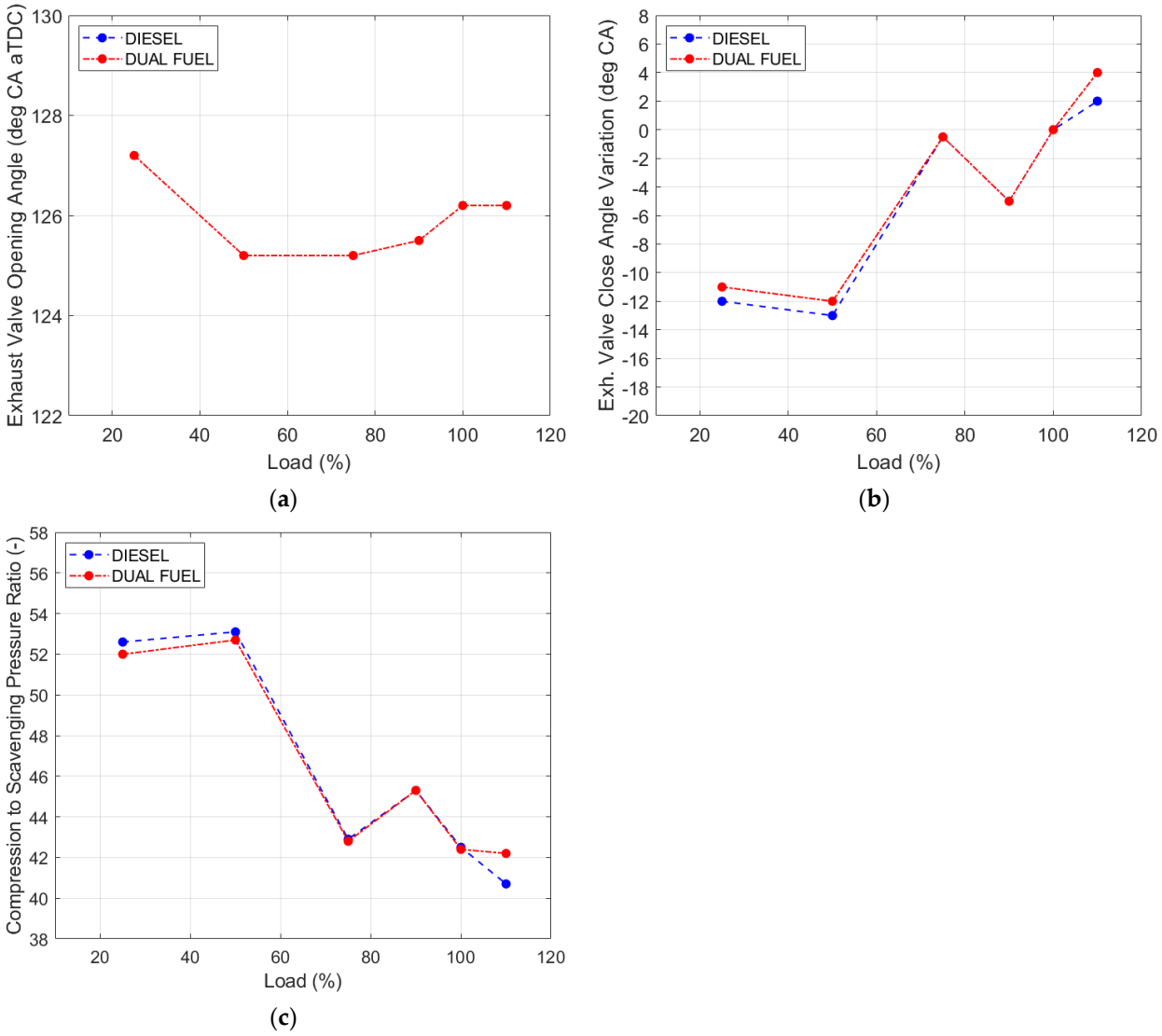

Figure 6. (**a**) Exhaust valve opening angle, diesel and DF modes; (**b**) Exhaust valve closing angle variation, diesel and DF modes; (**c**) Effective compression ratio (P_{comp}/P_{scav}), diesel and DF modes.

The main difference observed in the engine settings and the resulting performance for diesel and DF modes is the injection, and consequently, ignition timing. The liquid fuel injection timing, which is the ignition source, was estimated using the diagnostic software utilized for two-stroke diesel engine applications, described in Ref [26]. The ignition angle was estimated using two techniques for confidence, one based on the cumulative heat release diagram and a second based on the second derivative of cylinder pressure. Both methods provided essentially the same ignition angle in all examined cases, increasing the validity of the derived result. The point of combustion initiation was deemed to coincide with the ignition point of the diesel fuel. This assumption is valid and has been proven by various investigations, such as Refs [19,36–39]. In Figure 7a,b, the fuel (diesel mode) and diesel pilot (DF mode) injection angle and ignition angle are provided for all loads. The difference between the two figures is small due to the low value of diesel ignition delay. Fuel injection is advanced (before TDC) in the diesel mode up to the 75% load. Above that, the injection angle is retarded and remains almost steady. Advanced SOI has been found to provide efficiency advantages [40], while retarded SOI commonly results in lower NO_x emissions and also limits P_{max} values [41]. These are the main factors that affect engine tuning choices in this type of marine engine, and indeed, as shown in Figures 4b and 5f, the fuel efficiency and pressure increase are affected by SOI in the mid and high load regions.

On the other hand, in the DF mode, pilot injection is retarded (after TDC) under all loads. Despite the retarded SOI, the pressure rise due to combustion is comparable or higher than the diesel mode results. This is the first indication of a significantly more intense combustion in the DF mode, at least in the early (premixed) stage. For the 90% and 100% loads, the ignition angle is slightly advanced compared to the lower loads of this mode and is similar to the injection timing estimated for the diesel mode. The overall variation in liquid fuel injection timing is small, in the range of ±1° CA across all loads. For both modes, the injection timing of liquid fuel is generally retarded, close to or after TDC, to control the peak combustion pressure. Despite the difference in diesel fuel SOI timing, the peak combustion pressures were found nearly identical for all loads, as already shown in Figure 3a. This was attributed to the engine maker defining the SOI timing curves to have the same values of P_{max} for both modes and achieve similar performance. This is further elaborated in the combustion rate analysis section below and is mainly a result of the difference in the peak value of heat release between the two operating modes, as well as the premixed combustion rate difference.

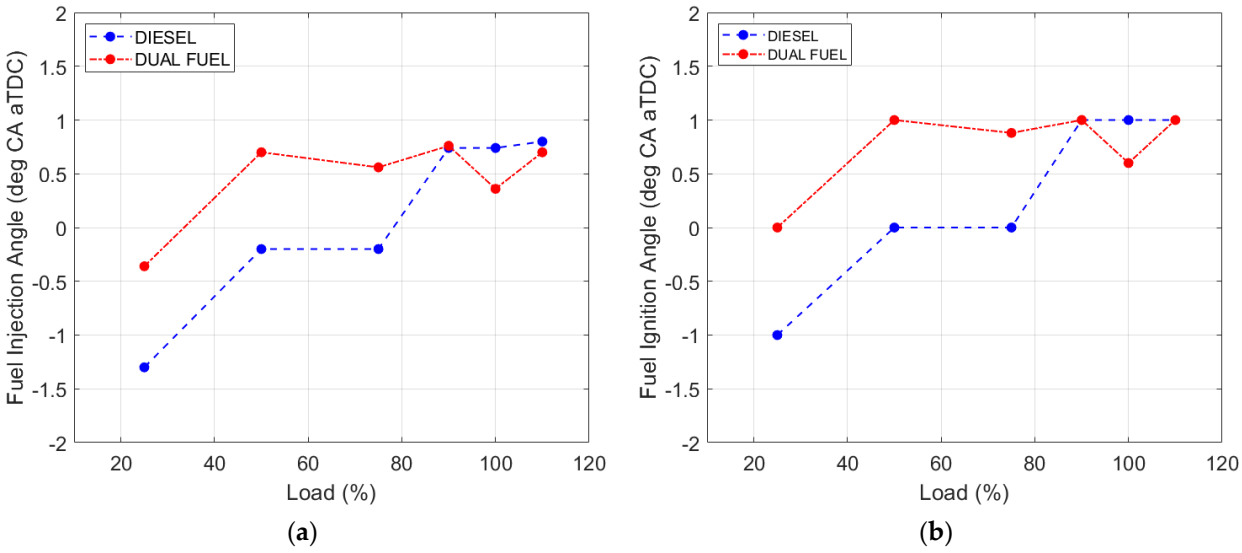

Figure 7. (**a**) Diesel injection angle, diesel and DF modes; (**b**) Diesel ignition angle, diesel and DF modes.

3.3. Measured Cylinder Pressure Traces and Combustion Rate Analysis

The measured cylinder pressure traces are shown in Figure 8 and compared between the diesel and DF modes for four of the six measured load points: 25%, 50%, 75% and 100% load. Based on the analysis of them, the net heat release rate diagrams were estimated and are provided for comparison. The calculated heat release rate diagrams (Figure 9) provide information on the evolution of the combustion process inside the combustion chamber. They are used for the estimation of the ignition angle, peak heat release rate, initial combustion slope and combustion duration. Utilizing this information, the overall combustion process can be comparatively evaluated from the early to the late stage.

In Figure 8a–d, the mean cylinder pressure traces for the diesel and DF modes are provided for 25% up to 100% loads. The overall differences are limited, as detailed in the previous section; differences are observed for the peak compression and combustion pressure and ignition angle. This is in line with the similarity in engine settings, apart from the fuel injection timing. The specific engine is ME-type technology, equipped with the auto-tuning system, which enables dynamic control of both P_{comp} and P_{max} on each cylinder, triggered by the cylinder pressure signal. After reviewing the cylinder pressure traces in the corresponding graphs, the tuning of the engine with the goal of achieving the same variation of P_{max} to load for both modes is made evident. This confirms that the specific DF marine engine design can provide similar performance under both DF and

diesel modes, which is not the case for all engine types when DF operation is tested [42]. This is an important finding in the present investigation.

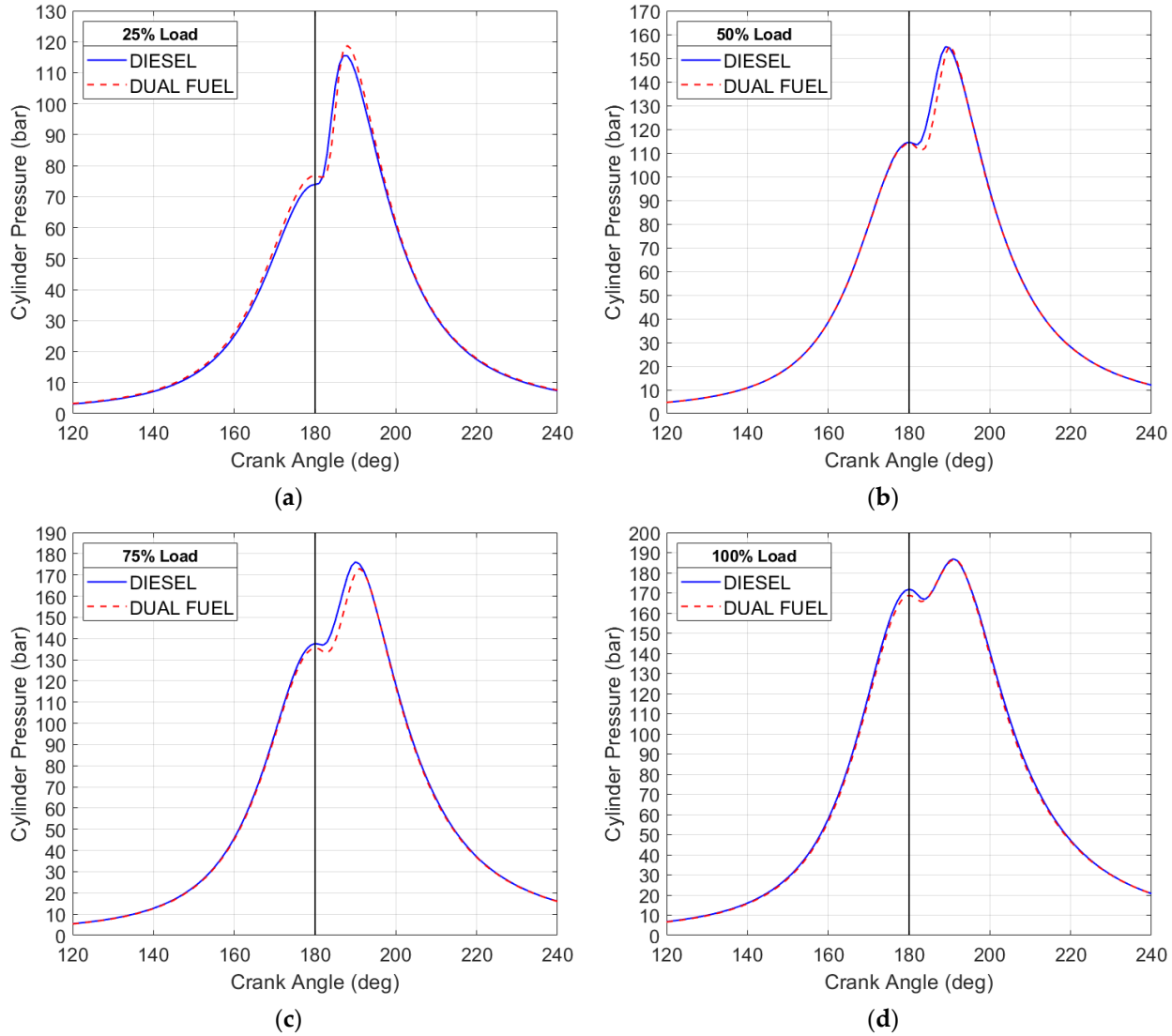

Figure 8. (**a**) Mean cylinder pressure traces at 25% load, diesel and DF modes; (**b**) Mean cylinder pressure traces at 50% load, diesel and DF modes; (**c**) Mean cylinder pressure traces at 75% load, diesel and DF modes; (**d**) Mean cylinder pressure traces at 100% load, diesel and DF modes.

In Figure 9a–d, the net heat release rate estimated from the mean cylinder pressure traces is presented for 25% up to 100% loads. In contrast to the cylinder pressure traces of Figure 8, the differences between diesel and DF modes are clear, especially in the low and medium load regions. This is an advantage of heat release rate analysis for engine performance and combustion investigation. From 25% to 75% load, the ignition occurs later for a DF mode operation, as expected, since both SOI timing and ignition delay are similar for both modes (Figure 7a,b). The peak value of heat release rate is considerably higher for the DF mode, with a maximum increase of 17.4% under a 50% load. This is in general agreement with similar studies of natural gas DF engines, such as Ref [35]. However, the reverse may also be encountered [20], mainly depending on the pilot ignition angle and the amount of diesel fuel injected [40]. The peak HRR difference, however, does not lead to a higher value of pressure rise due to combustion, which is about the same for both modes (Figure 4). Thus, the effect of the faster heat release rate for the DF mode is offset by the retarded ignition angle. In the case of the same ignition angle, the pressure rise due to

combustion would be significantly higher, and P_{max} would be expected to increase. The faster heat release rate is mostly attributed to fast mixing of the NG fuel and to its roughly 16.3% higher heating value. For a 90% load and above, the differences are minimized between the two operating modes, and the fuel ignition angle is similar; the 100% load results are provided in Figure 8d for reference. The same is observed for the peak value of heat release rate. This, again, reveals the ability of the injection system to supply fuel at the required rate even at full load. The physical properties of natural gas could potentially limit fuel mass delivery in the cylinder. However, this engine type and other modern NG engines inject natural gas at a low temperature and very high pressure, hence enabling a relatively high mass injection rate [7,12]. The relevant temperature and pressure values were measured at the site of tests, confirming previous findings. Despite similarities in the combustion rate for a 100% load (Figure 9d), the pressure rise due to combustion was higher in a DF mode operation (Figure 4b). This also applies to the 90% and 110% load points. For all tested loads, except 100%, late combustion was found to progress at a slightly slower rate under DF operation, despite later ignition in most cases. This is in conflict with the findings reported in Ref [42], where a better behavior of DF combustion in the late stages was observed.

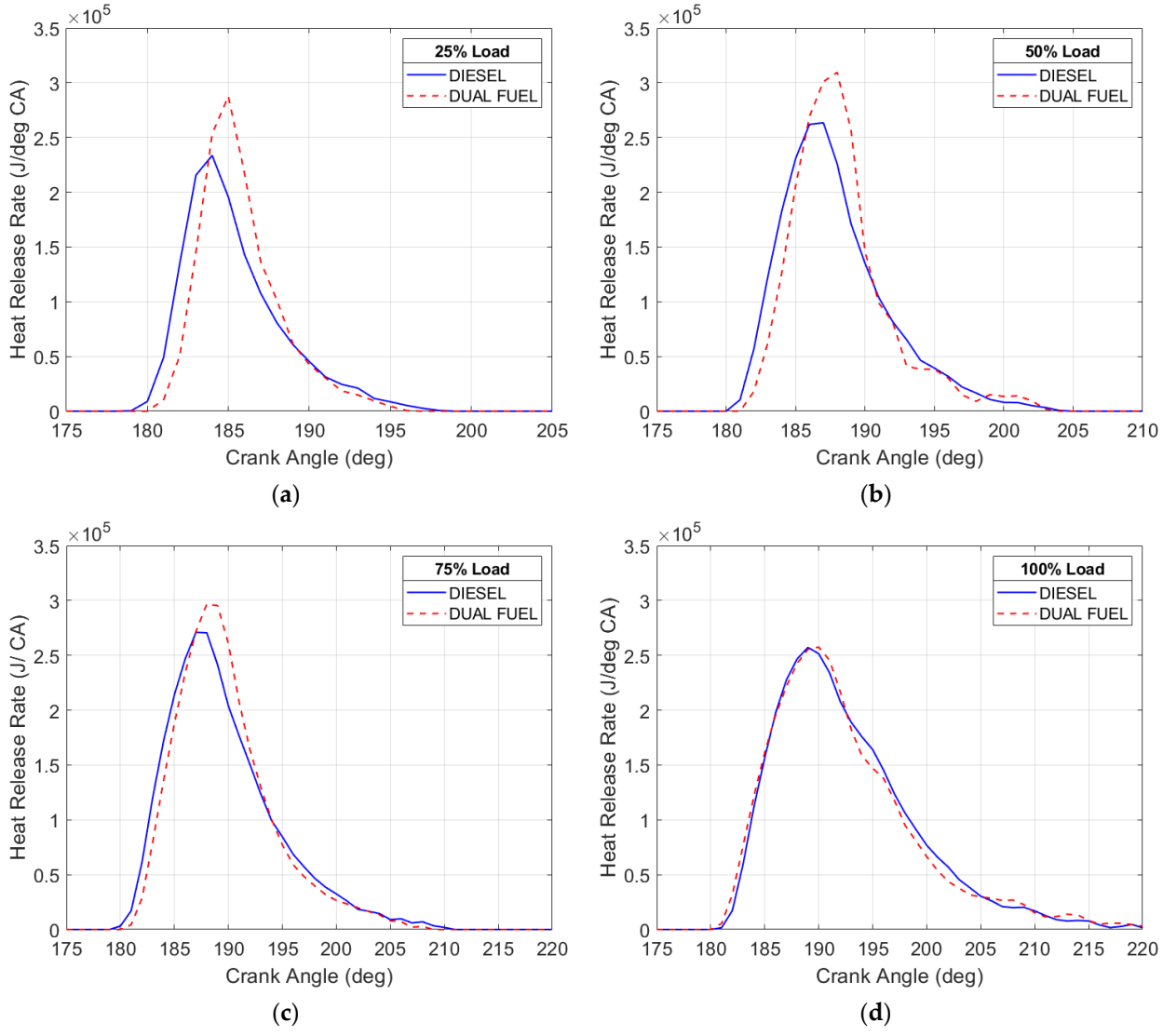

Figure 9. (**a**) Net mean heat release rate at 25% load, diesel and DF modes; (**b**) Net mean heat release rate at 50% load, diesel and DF modes; (**c**) Net mean heat release rate at 75% load, diesel and DF modes; (**d**) Net mean heat release rate at 100% load, diesel and DF modes.

Regarding natural gas fuel injection duration, the injection end can be estimated from Figure 9, as it occurs roughly at the angle of the HRR value. Figure 9 indicates that, for high load, the injection duration is similar to that of diesel fuel.

In addition to the differences in the progression rate of early stages, variations in diffusion-controlled and late-stage combustion can be observed. The observed differences in the HRR in a DF mode under low and mid loads of 25 to 75% (Figure 9a–c) lead to the assumption that the combustion process in a DF mode deviates further from the typical diesel mechanism when the ignition angle of pilot fuel is retarded, and the ratio of diesel/gas is high. It can be anticipated that these conditions could influence the premixed over the diffusion burn processes.

The combustion duration for 50% and 90% of total diesel and natural gas fuel mass fraction burnt was calculated, as already stated, using the cumulative heat release, which is the integral of Figure 9 diagrams' values. The results are provided in Figure 10. For the 25% up to 75% load and for both 50% and 90% of total fuel mass fraction burnt, early combustion progresses at a notably higher rate in a DF mode operation, indicated by the 6–8% shorter combustion duration. Due to the faster diffusion combustion, the difference increases further for 90% fuel combustion duration. The considerably shorter total combustion duration in the DF mode was also reported in Ref [22]. Usually, a shorter combustion duration results in efficiency benefits, as thermal losses are also limited. In the present case, this is observed under the 25% load. The SOI delay of the pilot diesel fuel in the DF mode is possibly the major reason for the small efficiency loss of 1%. The near maximum load premixed phase combustion rate is similar for both modes. The late combustion stage progresses more slowly in the DF mode, which contrasts with the expectations based on Ref [39], which is, however, based only on simulation results of a marine four-stroke propulsion engine. This highlights the importance of experimental data use on actual scale engines of the two-stroke variant. The slower late combustion under full load affects combustion duration, which is equal or slightly longer than that of the diesel mode, in contrast to the shorter duration observed under lower loads. This is found by examining both the 50% and 90% total fuel burnt. The difference in the total heat release between the two modes that can be observed in some cases is attributed to the slight load differences and variation in heat losses.

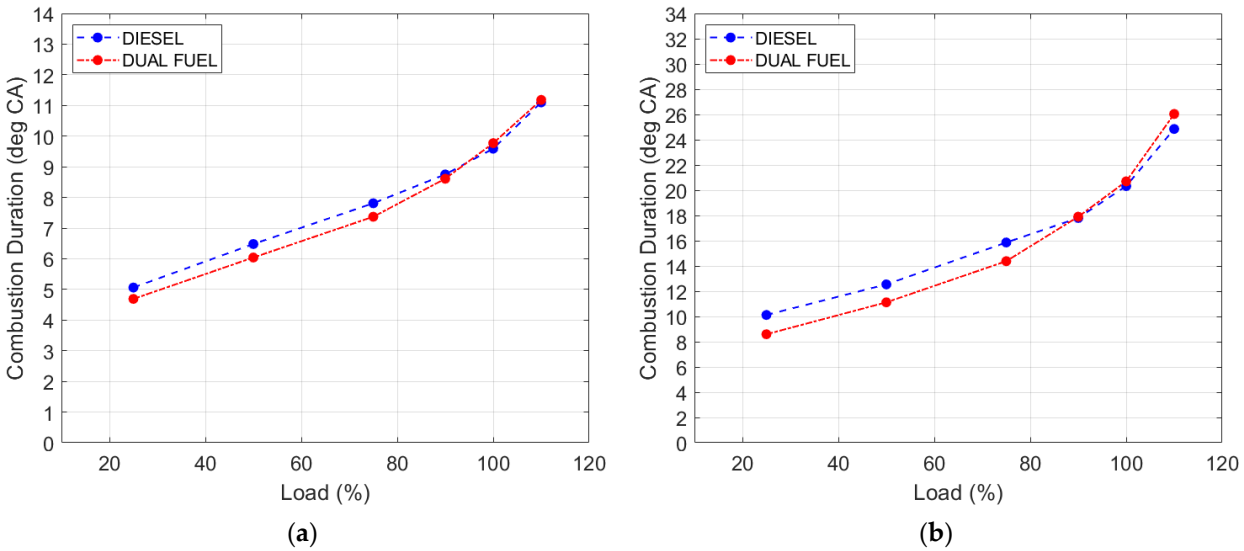

Figure 10. (**a**) Combustion duration for 50% fuel mass fraction burnt, diesel and DF modes; (**b**) Combustion duration for 90% fuel mass fraction burnt, diesel and DF modes.

4. Summary and Conclusions

In the present study, the performance of a two-stroke marine diesel engine operating under the high-pressure natural gas injection principle was examined for both DF and

diesel modes. The comparative evaluation revealed that, overall, limited differences were observed between the two modes for the specific engine design. The engine settings regarding exhaust valve timing were found to be nearly identical for the opening angle, with differences observed only for the closing angle at low and high loads. For the diesel injection (pilot in the case of DF operating mode) and, consequently, ignition angle, differences up to 1° crank angle for low and mid loads, with retarded injection timing for the DF mode, were observed. This is an important finding, since multiple studies have shown that the injection angle has a major effect on pressure rise and on the overall evolution of the combustion process [41,43]. The main performance data were found to be similar, and the only difference of note was observed in the pressure increase due to combustion influenced by the SOI angle and combustion intensity under a DF mode due to the NG high LCV. The combustion process analysis revealed differences mainly for low and medium loads. The combustion rate was more intense in a DF operation and presented a higher peak rate, similar to the findings of Refs [35,40] for which the SOI under a DF mode was also retarded. Increased combustion intensity was attributed to the higher LCV of injected natural gas and the better mixing of gas and air until the diesel pilot ignition. The same was observed for most of the diffusion-controlled combustion process, attributed to the fast ignition [19] of NG inside the combustion chamber. A prerequisite for the former was the ability of the NG fuel supply system to inject a high mass of gaseous fuel in the combustion chamber at a rate comparable to diesel. This was confirmed by the HRR diagrams, as the time from ignition to peak HRR, where injection is approximately considered to terminate, was similar or lower in the DF mode. Late-stage combustion also progressed slightly faster in the DF operation. The faster burn rate resulted in lower combustion duration under the DF mode for these loads for both 50% and 90% fuel mass fraction burnt. The aforementioned differences were not observed under high loads, with the HRR being mostly identical. Based on these differences, it can be estimated that the combustion process in DF mode deviates from the typical diesel mechanism when the ignition angle of pilot fuel is retarded, and the ratio of diesel to natural gas is high, by affecting the intensity of premixed and diffusion burn processes. The power output remained the same in both modes due to the higher heating value of the NG fuel and its adequate mass injection rate because of the high injection pressure. SFC in the diesel mode was lower overall when expressed in terms of the total heat rate provided by the supplied fuel, signifying better overall thermal efficiency. The difference between the two modes was in the range of 1–2%. This is promising, considering the known positive effect of dual fuel operation on CO_2 emissions [5]. Regarding CO_2 emissions, the overall effect was a 22.6% improvement despite the efficiency reduction, as the carbon content of natural gas was 12% lower than diesel while also providing 16.3% higher energy content, which resulted in lower total fuel mass consumed. Detailed analysis on the emissions, including NO_x emissions and the measurement data during EGR use, will be presented in a future study.

Overall, the use of a high-pressure system for natural gas injection resulted in operation and efficiency very close to that of a typical diesel cycle without extensive settings changes, mainly regarding injection timing. The main performance values were almost identical, excluding the limited differences in efficiency, which was optimized for low–medium load operation for DF mode and was increased but sufficiently close to that of the diesel mode for other loads. This reveals that modern marine two-stroke high-pressure DF engine performance can be very close to the standards of a diesel-only operation while providing concrete environmental benefits in terms of CO_2 emissions.

Author Contributions: Conceptualization, T.D.H. and T.C.Z.; methodology, T.D.H.; validation, T.D.H.; investigation, T.D.H.; writing—review and editing, T.C.Z. and M.F.; supervision, M.F. All authors have read and agreed to the published version of the manuscript.

Funding: This research received no external funding.

Data Availability Statement: Data used in the specific study are not publicly archived. The measurement data used for analysis are the property of the owner of the vessel equipped with the tested engine and are confidential.

Conflicts of Interest: The authors declare no conflict of interest.

Nomenclature

Abbreviations	
CFD	Computational Fluid Dynamics
DF	Dual Fuel
ECS	Engine Control System
EGR	Exhaust Gas Recirculation
EMS	Engine Monitoring System
EVC	Exhaust Valve Closing
EVO	Exhaust Valve Opening
FAT	Factory Acceptance Test
HRR	Heat Release Rate
IMO	International Maritime Organization
LCV	Lower Calorific Value
LNG	Liquified Natural Gas
MOP	Main Operating Panel
NG	Natural Gas
P_{comp}	Compression Pressure
P_{max}	Maximum Combustion Pressure
P_{scav}	Scavenging Pressure
PMI	Pressure Mean Indicator
SFC	Specific Diesel Fuel Consumption
SGC	Specific Gas Fuel Consumption
SPC	Specific Pilot Diesel Fuel Consumption
SOI	Start of Injection
TDC	Top Dead Center
THR	Total Heat Rate
Symbols	
A	Surface Area (m^2)
a_c	Coefficient Constant (-)
b	Coefficient Constant (-)
c_r	Coefficient Constant (W/m^2K^4)
c_v	Specific Heat at Constant Volume (J/kgK)
D	Cylinder Bore (m)
R	Gas Constant (J/kg·K)
Re	Reynolds Number
P	Pressure (Pa)
V	Volume (m^3)
$Q_{net/gross}$	Heat Release Gross/Net (J)
Q_w	Heat Loss (J)
m	Mass (kg)
T	Temperature (K)
Greek Symbols	
λ	Gas Thermal Conductivity (W/m·K)
φ	Crank Angle (deg)
Subscripts	
g	Gas
w	Wall

References

1. Chircop, A. The IMO Initial Strategy for the reduction of GHGs from international shipping: A Commentary. *Int. J. Mar. Coast. Law* **2019**, *34*, 482–512. [CrossRef]
2. Yusuf, A.A.; Inambao, F.L.; Ampah, J.D. Evaluation of biodiesel on speciated PM2.5, organic compound, ultrafine particle and gaseous emissions from a low-speed EPA Tier II marine diesel engine coupled with DPF, DEP and SCR filter at various loads. *Energy* **2022**, *239*, 121837. [CrossRef]
3. Yusuf, A.A.; Yusuf, D.A.; Jie, Z.; Bello, T.Y.; Tambaya, M.; Abdullahi, B.; Muhammed-Dabo, I.A.; Yahuza, I.; Dandakouta, H. Influence of waste oil-biodiesel on toxic pollutants from marine engine coupled with emission reduction measures at various loads. *Atmos. Pollut. Res.* **2022**, *13*, 101258. [CrossRef]
4. Thomson, H.; Corbett, J.J.; Winebrake, J.J. Natural gas as a marine fuel. *Energy Policy* **2015**, *87*, 153–167. [CrossRef]
5. DNV. Maritime Forecast to 2050-Energy Transition Outlook 2021. *DNV* **2021**, *118*.
6. Jin, S.Y.; Li, J.Z.; Zi, Z.Y.; Liu, Y.L.; Wu, B.Y. Effects of different combustion modes on the thermal efficiency and emissions of a diesel pilot-ignited natural gas engine under low-medium loads. *J. Cent. South Univ.* **2022**, *29*, 2213–2224. [CrossRef]
7. Boretti, A. Advances in diesel-LNG internal combustion engines. *Appl. Sci.* **2020**, *10*, 1296. [CrossRef]
8. Huan, T.; Hongjun, F.; Wei, L.; Guoqiang, Z. Options and evaluations on propulsion systems of LNG carriers. In *Propulsion Systems*; Serpi, A., Porru, M., Eds.; IntechOpen: Rijeka, Yugoslavia, 2019. [CrossRef]
9. Abadie, L.M.; Goicoechea, N. Powering newly constructed vessels to comply with ECA regulations under fuel market prices uncertainty: Diesel or dual fuel engine? *Transp. Res. Part D Transp. Environ.* **2019**, *67*, 433–448. [CrossRef]
10. International Maritime Organization. *NOx Technical Code 2008, Technical Code on Control of Emission of Nitrogen Oxides from Marine Diesel Engines*; International Maritime Organization: London, UK, 2008.
11. American Burau of Shipping (ABS). *ABS Advisory on NOx Tier III Compliance*; ABS: Spring, TX, USA, 2020.
12. MAN Diesel & Turbo. MAN B&W ME-GI Dual-Fuel, Low-Speed Engine 2016. Available online: https://mandieselturbo.com/docs/default-source/shopwaredocuments/man-b-w-me-giee40ba7d787543c688da0d9c11628006.pdf?sfvrsn=3 (accessed on 5 December 2022).
13. Boretti, A. Numerical Analysis of high-pressure direct injection dual-fuel diesel-liquefied natural gas (LNG) engines. *Processes* **2020**, *8*, 261. [CrossRef]
14. Ott, M.; Winterthur, G.D.; Ingemar Nylund, I.A.; Roland Alder, W.G.D.L.; Takayuki Hirose, I.C.; Yoshiyuki Umemoto, D.U.L.; Takeshi Yamada, I.C. *The 2-Stroke Low-Pressure Dual-Fuel Technology: From Concept to Reality*; CIMAC: Helsinki, Finland, 2016; Volume 95, pp. 46–50.
15. Stoumpos, S.; Theotokatos, G.; Mavrelos, C.; Boulougouris, E. Towards marine dual fuel engines digital twins-integrated modelling of thermodynamic processes and control system functions. *J. Mar. Sci. Eng.* **2020**, *8*, 220. [CrossRef]
16. Gürbüz, H.; Demirtürk, S.; Akçay, İ.H.; Akçay, H. Effect of port injection of ethanol on engine performance, exhaust emissions and environmental factors in a dual-fuel diesel engine. *Energy Environ.* **2020**, *32*, 784–802. [CrossRef]
17. Akçay, I.H.H.; Gürbüz, H.; Akçay, H.; Aldemir, M. An investigation of euro diesel-hydrogen dual-fuel combustion at different speeds in a small turbojet engine. *Aircr. Eng. Aerosp. Technol.* **2021**, *93*, 701–710. [CrossRef]
18. Imhoff, T.B.; Gkantonas, S.; Mastorakos, E. Analysing the performance of ammonia powertrains in the marine environment. *Energies* **2021**, *14*, 7447. Available online: https://www.mdpi.com/1996-1073/14/21/7447/htm (accessed on 10 April 2023). [CrossRef]
19. Nemati, A.; Ong, J.C.; Pang, K.M.; Mayer, S.; Walther, J.H. A numerical study of the influence of pilot fuel injection timing on combustion and emission formation under two-stroke dual-fuel marine engine-like conditions. *Fuel* **2022**, *312*, 122651. [CrossRef]
20. Yang, R.; Theotokatos, G.; Vassalos, D. CFD modelling and numerical investigation of a large marine two-stroke dual fuel direct injection engine. *Ships Offshore Struct.* **2022**, *17*, 1062–1074. [CrossRef]
21. Hountalas, D.T.; Papagiannakis, R. Theoretical and experimental investigation of a direct injection dual fuel diesel-natural gas engine. *SAE Tech. Pap.* **2002**, *19*. [CrossRef]
22. Yu, H.; Wang, W.; Sheng, D.; Li, H.; Duan, S. Performance of combustion process on marine low speed two-stroke dual fuel engine at different fuel conditions: Full diesel/diesel ignited natural gas. *Fuel* **2022**, *310*, 122370. [CrossRef]
23. Arefin, M.A.; Nabi, M.N.; Akram, M.W.; Islam, M.T.; Chowdhury, M.W. A review on liquefied natural gas as fuels for dual fuel engines: Opportunities, challenges and responses. *Energies* **2020**, *13*, 6127. [CrossRef]
24. Figari, M.; Theotokatos, G.; Coraddu, A.; Stoumpos, S.; Mondella, T. Parametric investigation and optimal selection of the hybrid turbocharger system for a large marine four-stroke dual-fuel engine. *Appl. Therm. Eng.* **2022**, *208*, 117991. [CrossRef]
25. Stoumpos, S.; Theotokatos, G. A novel methodology for marine dual fuel engines sensors diagnostics and health management. *Int. J. Engine Res.* **2022**, *23*, 974–994. [CrossRef]
26. Hountalas, D.T.; Papagiannakis, R.G. Development of a simulation model for direct injection dual fuel diesel-natural gas engines. *SAE Tech. Pap.* **2000**, *13*. [CrossRef]
27. MAN Energy Solutions. Technical Documentation Project Guide G70ME-C9.5-GI [Internet]. Copenhagen: MAN Energy Solutions. 2020. Available online: https://man-es.com/applications/projectguides/2stroke/content/printed/G70ME-C9_5-GI.pdf (accessed on 5 February 2023).

28. Hountalas, D.T.; Papagiannakis, R.G.; Zovanos, G.; Antonopoulos, A. Comparative evaluation of various methodologies to account for the effect of load variation during cylinder pressure measurement of large scale two-stroke diesel engines. *Appl. Energy* **2014**, *113*, 1027–1042. [CrossRef]
29. Papagiannakis, R.; Hountalas, D. Combustion and exhaust emission characteristics of a dual fuel compression ignition engine operated with pilot Diesel fuel and natural gas. *Energy Convers. Manag.* **2004**, *45*, 2971–2987. [CrossRef]
30. Kouremenos, D.A.; Rakopoulos, C.D.; Hountalas, D.T. Multi-zone combustion modelling for the prediction of pollutants emissions and performance of DI diesel engines. *SAE Trans. J. Engines* **1997**, *106*, 940–957. [CrossRef]
31. Hardenberg, H.O.; Hase, F.W. An empirical formula for computing the pressure rise delay of a fuel from its cetane number and from the relevant parameters of direct-injection diesel engines. *SAE Trans.* **1979**, *88*, 1823–1834.
32. Heywood, J.B. *Internal Combustion Engine Fundamentals*; McGraw-Hill: New York, NY, USA, 1988; Volume 26. [CrossRef]
33. Thermodynamics and Fluid Mechanics Group; Annand, W.J.D. Heat transfer in the cylinders of reciprocating internal combustion engines. *Proc. Inst. Mech. Eng.* **1963**, *177*, 973–996. [CrossRef]
34. Yu, H.; Duan, S.; Sun, P. Comparative analysis between natural gas/diesel (dual fuel) and pure diesel on the marine diesel engine. *J. Eng. Res.* **2015**, *3*, 111–125. [CrossRef]
35. Lounici, M.S.; Loubar, K.; Tarabet, L.; Balistrou, M.; Niculescu, D.C.; Tazerout, M. Towards improvement of natural gas-diesel dual fuel mode: An experimental investigation on performance and exhaust emissions. *Energy* **2014**, *64*, 200–211. [CrossRef]
36. Xu, S.; Anderson, D.; Hoffman, M.; Prucka, R.; Filipi, Z. A phenomenological combustion analysis of a dual-fuel natural-gas diesel engine. *Proc. Inst. Mech. Eng. Part D J. Automob. Eng.* **2017**, *231*, 66–83. [CrossRef]
37. Larson, C.R. Injection Study of a Diesel Engine Fueled with Pilot-Ignited, Directly-Injected Natural Gas. Master's Thesis, University of British Columbia, Vancouver, BC, Canada, 2003.
38. Naber, J.D.; Siebers, D.L.; Di Julio, S.S.; Westbrook, C.K. Effects of natural gas composition on ignition delay under diesel conditions. *Combust. Flame* **1994**, *99*, 192–200. [CrossRef]
39. Liu, H.; Li, J.; Wang, J.; Wu, C.; Liu, B.; Dong, J.; Liu, T.; Ye, Y.; Wang, H.; Yao, M. Effects of injection strategies on low-speed marine engines using the dual fuel of high-pressure direct-injection natural gas and diesel. *Energy Sci. Eng.* **2019**, *7*, 1994–2010. [CrossRef]
40. Li, M.; Zhang, Q.; Li, G.; Shao, S. Experimental investigation on performance and heat release analysis of a pilot ignited direct injection natural gas engine. *Energy* **2015**, *90*, 1251–1260. [CrossRef]
41. Guo, H.; Zhou, S.; Zou, J.; Shreka, M. A Numerical Study on the Pilot Injection Conditions of a Marine 2-Stroke Lean-Burn Dual Fuel Engine. *Processes* **2020**, *8*, 1396. Available online: https://www.mdpi.com/journal/processes (accessed on 8 April 2023). [CrossRef]
42. Pham, V.C.; Choi, J.H.; Rho, B.S.; Kim, J.S.; Park, K.; Park, S.K.; Le, V.V.; Lee, W.-J. A numerical study on the combustion process and emission characteristics of a natural gas-diesel dual-fuel marine engine at full load. *Energies* **2021**, *14*, 1342. Available online: https://www.mdpi.com/1996-1073/14/5/1342/htm (accessed on 7 April 2023). [CrossRef]
43. Sun, L.; Liu, Y.; Zeng, K.; Yang, R.; Hang, Z. Combustion performance and stability of a dual-fuel diesel-natural-gas engine. *Proc. Inst. Mech. Eng. Part D J. Automob. Eng.* **2015**, *229*, 235–246. Available online: https://journals.sagepub.com/doi/abs/10.1177/0954407014537814?journalCode=pidb (accessed on 8 April 2023). [CrossRef]